

Research Article

DFT/TDDFT and Experimental Studies of Natural Pigments Extracted from Black Tea Waste for DSSC Application

N. T. R. N. Kumara, Muhammad Raziq Rahimi Kooh, Andery Lim, Mohammad Iskandar Petra, Nyuk Yoong Voo, Chee Ming Lim, and Piyasiri Ekanayake

Applied Physics Program, Faculty of Science, Universiti Brunei Darussalam, Jalan Tungku Link, Gadong BE1410, Brunei Darussalam

Correspondence should be addressed to Piyasiri Ekanayake; piyasiri.ekanayake@ubd.edu.bn

Received 21 May 2013; Revised 9 August 2013; Accepted 11 August 2013

Academic Editor: Vincenzo Augugliaro

Copyright © 2013 N. T. R. N. Kumara et al. This is an open access article distributed under the Creative Commons Attribution License, which permits unrestricted use, distribution, and reproduction in any medium, provided the original work is properly cited.

We report results of combined experimental and theoretical studies of black tea waste extract (BTE) as a potential sensitizer for TiO₂-dye-sensitized solar cells (DSSCs). UV-vis absorption data revealed that BTE contains theaflavin. DSSC sensitized with pigment complexes of BTE showed a photon-energy conversion efficiency of $\eta = 0.20\%$, while a significant increase ($\eta = 0.46\%$) is observed when pH of the pigment solution was lowered. The HOMO and LUMO energy levels were calculated using experimental data of UV-vis absorption and cyclic voltammetry. These calculations revealed a reduction of the band gap by 0.17 eV and more negativity of HOMO level of acidified pigment, compared to that of original pigment. Combined effect of these developments caused the enhanced efficiency of DSSC. Density functional theory (DFT) and time-dependent density functional theory (TDDFT) computational calculations were carried out to study the four theaflavin analogues which are responsible for the dark colour of BTE. According to the calculations, two theaflavin analogues, theaflavin and theaflavin digallate, are the most probable sensitizers in this dye-sensitized solar cell system.

1. Introduction

Dye-sensitized solar cells (DSSCs) are devices that convert visible light into electricity based on the photosensitization of wide band gap metal oxide semiconductors and have attracted wide interest as a low cost solar energy conversion device [1] and thus towards the development and improvement of new families of dyes and metal complexes [1, 2]. It is one of the most promising new generation systems for photovoltaic technology and has emerged as one of renewable energy sources as a result of exploiting several new concepts and materials, such as nanotechnology and molecular devices.

This DSSC device is based on chemical concepts, in which the separation of charge carriers is kinetically controlled by the reactions involved [3]. Most of the efficient DSSCs are sensitized with the dyes having ruthenium based complexes that have been shown to operate with power conversions around 11% using nanoporous TiO₂ electrodes. However,

due to the high cost of ruthenium complexes and the long-term unavailability of these noble metals [4], there is a need to search for alternative photosensitizers for the use in TiO₂-based photovoltaic devices.

Multistep procedures in the preparation and development of synthetic dyes as sensitizers of DSSC normally involve variety of solvents and time consuming purification processes, thus making synthetic dye production not only very expensive but also environmentally unfriendly [5]. Several studies have found possibilities of using natural dyes as DSSC's sensitizer. DSSCs equipped with natural dyes as sensitizers have several advantages over rare metal complexes and other synthetic dyes [6] that they can easily be extracted from fruits, vegetables, and flowers with minimal chemical procedures, thus attracting a great interest in producing low cost sensitizers [7].

The availability in large quantities, convenient extraction into cheap organic solvents, ability of application without

fine purification, and environmentally-friendly and low production cost of the devices are some of the competitive advantages of the natural dyes. The highest overall solar energy conversion efficiency, reported in literature, is around 2% when DSSCs were sensitized with natural pigments [8, 9].

Other antioxidant components, which absorb light within the visible regions such as phenolic compounds (flavonoids) and tannins, are also known to be able to adsorb onto TiO_2 strongly [1]. These components can be found also in tea. The constituents of black tea are particularly dominated by polyphenols called catechins [10] with some other phenolic acids, flavanols such as theaflavins, rutin, and some nonprotein amino acids called theanine [11].

Black tea has a yellow-orange colouration which accounts for the presence of theaflavins (TFs) and thearubigins [12]. TFs include theaflavin (TF), theaflavin-3-gallate (T3G), theaflavin-3'-gallate (T3'G), and theaflavin digallate (TDG) which are phenolic compounds resulted from the oxidation of the tea catechin [13]. Theaflavin (Figure 1) is golden yellow in color [14] and has been identified to be responsible for making a considerable brightness of black tea infusion as reported by Liang and Xu [15]. These polyphenolic compounds presence in tea has the capability to absorb light in the visible region, worth investigating their potential as sensitizers in DSSC. Moreover, there is currently no study of using tea pigments as sensitizers [16].

Through this study, the waste of black tea extract, which we labelled as BTE, has been found useful and has the potential to be utilized as a sensitizer of DSSC. The experimental studies are limited to using the pigments from the tea extract as a whole, and no separation of the pigments was carried out. Computational modeling was carried out to provide further understanding of the energy levels, the simulated absorption spectra, and the electron clouds of four pigments found in black tea.

2. Experimental

2.1. Fabrication of Working Electrode. Photoelectrodes were fabricated using a TiO_2 paste Solaronix (nanoxide-T, colloidal anatase particles size: ~ 13 nm, ~ 120 m² g⁻¹ (BET), Switzerland). The TiO_2 was coated on precleaned fluorine-doped conducting tin oxide (FTO) glasses (Nippon sheet glass 10–12 Ω sq⁻¹) by Doctor Blade method. Electrodes were preheated ($\sim 50^\circ\text{C}$) using a hair drier and sintered at 450°C for 30 minutes. The thickness of the TiO_2 electrodes used for this investigation was ~ 9 μm (Dektak profilometer; Veeco, Dektak 3) [7].

2.2. Pigment Extraction. The collected black tea waste was recovered to about 10 grams of dry sample. The dye pigment complex was extracted by crushing it with a minimum amount of 70% ethanol (diluted from Scharlau 99.9% absolute ethanol with distilled water). The residual solids were filtered off, and the extract was then centrifuged to separate any remaining solid content. The presence of visible light absorbing component in the black tea extract was confirmed

by using the UV-vis absorption spectroscopy (Shimadzu UV-1800) [17]. The tea waste extract of different pH values (pH = 2.5, 3.5, 4.5, and 7) were prepared by adding 0.1 M HCl and 0.1 M NaOH solutions to original BTE (Thermo Scientific, Orion Star A211).

2.3. Dye-Sensitized Solar Cell Preparation. The TiO_2 electrodes were subsequently dipped in the extracted black tea for 14 hours [18, 19]. The electrodes were then removed, rinsed with absolute ethanol, and air-dried. DSSCs were assembled by introducing the redox electrolyte containing tetrabutylammonium iodide (TBAI; 0.5 M)/ I_2 (0.05 M), in a mixture of acetonitrile and ethylene carbonate (6:4, v/v) between the dyed TiO_2 electrode and platinum counter electrode [7]. Those DSSCs were placed under irradiation of 1000 W/m² about 4–6 hours after applying the electrolyte to obtain the best current, possibly due to slow incorporation of electrolyte into TiO_2 layer.

2.4. Cyclic Voltammetry Measurements. Cyclic voltammetry (CV) measurements were carried out using eDAQ potentiostat, equipped with e-corder 401 and eDAQ software EChem version 2.1.5. A three-electrode system consisting of a glassy carbon working electrode, platinum counter electrode, and 4 M KCl saturated Ag/AgCl reference electrode was used. The scanning range of the CV was between -1000 mV and $+1000$ mV, at a scan rate of 50 mV/s, and at the starting potential of -1000 mV. 20 μL of the required dye solutions was separately placed on the glassy carbon working electrode and allowed to dry at room temperature before immersing the electrode in supporting electrolyte. The supporting electrolyte was 0.1 M KNO_3 .

2.5. Computational Studies. The molecular structures of TFs were computed using Spartan'10 software [20] to retrieve the molecular geometric coordinates. Both density functional theory (DFT) and time-dependent density functional theory (TDDFT) calculations were performed using Gaussian 09W software [21]. B3LYP hybrid functional and 6-31g(d) basis set were used as calculation methods. All the calculations include solvation effect in ethanol. The models of electron density of various energy levels of the TFs were visualized using GaussView Version 5.0 [22].

3. Results and Discussion

3.1. Optical Properties. UV-vis absorption spectra of BTE are depicted in Figure 2(a). UV-vis analysis showed an absorption peak appearing around 372 nm in original BTE (pH of original BTE is 5.65), while the peak shifted narrowly to the left, and an additional peak appeared around 420 nm when BET was acidified (pH = 3.5). These absorption peaks are due to the presence of theaflavin in the tea waste extract [23]. According to the DFT computational values of the tea pigments, the λ_{max} of TF, T3G, T3'G, and TDF were at 458 nm, 439 nm, 440 nm, and 461 nm, respectively (Figure 2(b)), and these peaks were observed also in Figure 2(a).

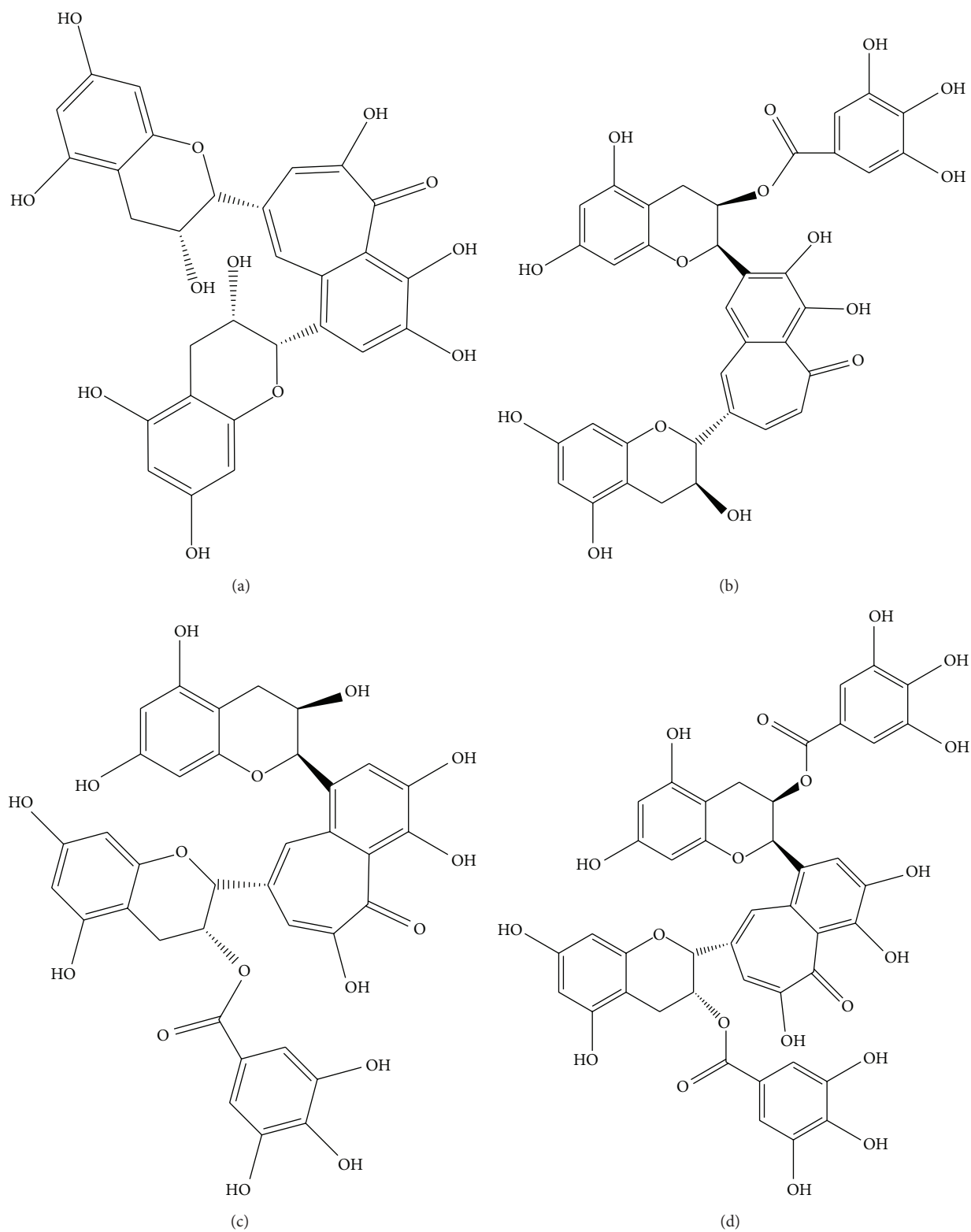


FIGURE 1: Molecular structure of black tea pigments: (a) theaflavin (TF), (b) theaflavin-3-gallate (T3G), (c) theaflavin-3'-gallate (T3'G), and (d) theaflavin Digallate (TDG).

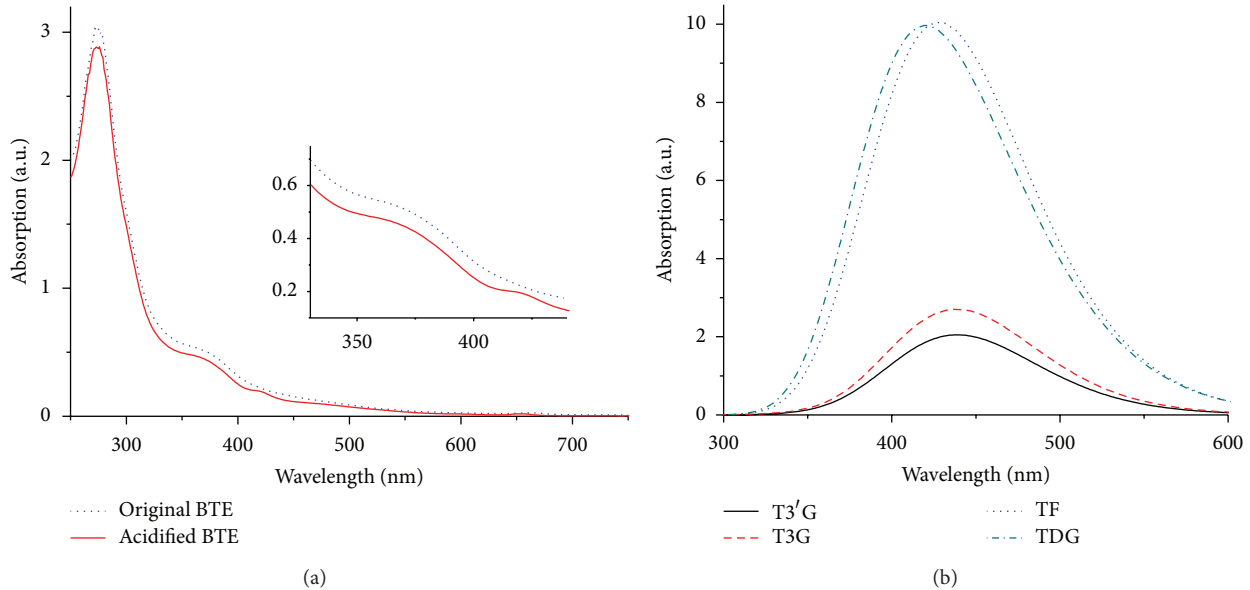


FIGURE 2: (a) UV-vis absorption spectra of BTE pigments (original and acidified pigment). Inset shows an enlarged picture of the emerging absorption peak. (b) Simulated UV-vis absorption spectra obtained for the four TF analogues obtained via TDDFT calculation.

The optical band gap of the pigment was calculated by employing the Tauc method [24–27]. Values of optical band were determined by the extrapolation of the linear region to zero absorbance from a plot that was drawn according to the Tauc relation when $n = 1/2$

$$A h \nu \approx (h \nu - E_g)^n, \quad (1)$$

where A is absorbance, E_g is band gap, and $h \nu$ is photon energy.

Plots of $(A h \nu)^2$ versus $h \nu$ were illustrated in Figures 3(a) and 3(b) for the original pigment and the pigment at lowered pH, respectively. The calculated optical band gaps of original pigment and after HCl treatment were 2.97 eV and 2.80 eV, respectively (Table 1). The band gap of acidified BTE was reduced compared to that of original BTE, which is favorable for efficient absorption of solar energy.

3.2. Electrochemical Properties. The electrochemical behavior of the pigment was investigated by using cyclic voltammetry (CV). The study shows further possibilities of electron injection from the excited state of dye pigment to conduction band of semiconductor and the dye regeneration ability. The cyclic voltammograms of the original and acidified BTE pigments are shown in Figure 4. The first oxidation potential of pigment is corresponding to HOMO level of dye pigment. The HOMO levels of original and acidified pigments of BTE were observed to be 0.28 eV and 0.35 eV (versus Ag/AgCl), respectively [28]. Table 1 shows HOMO and LUMO energy levels of BTE pigment with respect to vacuum. The HOMO level is a major factor of electron donor mechanism. The electron donating ability will decrease when HOMO is more positive. According to our experimental values of HOMO levels, acidified BTE has more donating ability compared with original BTE pigment.

TABLE 1: Calculated HOMO and LUMO energy levels and band gaps of BTE.

Sample	HOMO (eV)	LUMO (eV)	Band gap (eV)
BTE	-4.68	-1.71	2.97
Acidified BTE	-4.75	-1.95	2.80

All energy values are with respect to the vacuum level.

3.3. Photovoltaic Characterization. Figure 5 shows I - V (current-voltage) characteristics of the DSSCs sensitized with BTE pigment. Table 2 presents the performance of the DSSCs in terms of short circuit current density (I_{SC}), open circuit voltage (V_{OC}), fill factor (ff), and energy conversion efficiency (η) for original and acidified BTE.

The maximum power conversion efficiency was calculated using the following formula:

$$\eta = \frac{I_{SC} \cdot V_{OC} \cdot \text{ff}}{P}. \quad (2)$$

Here, P is the intensity of the incident light.

The fill factor (ff) was defined as the ratio of the maximum power P_{\max} obtained from the DSSC and the theoretical maximum power of it.

Hence,

$$\text{ff} = \frac{I_m \cdot V_m}{I_{SC} \cdot V_{OC}}. \quad (3)$$

Here, I_m and V_m are current and voltage related to the maximum power.

The DSSCs sensitized with BTE showed a conversion efficiency (η) of 0.20%, with open circuit voltage (V_{OC}) of 434 mV short circuit current density (I_{SC}) of 0.82 mA cm⁻², and fill factor (ff) of 0.57. This performance was further

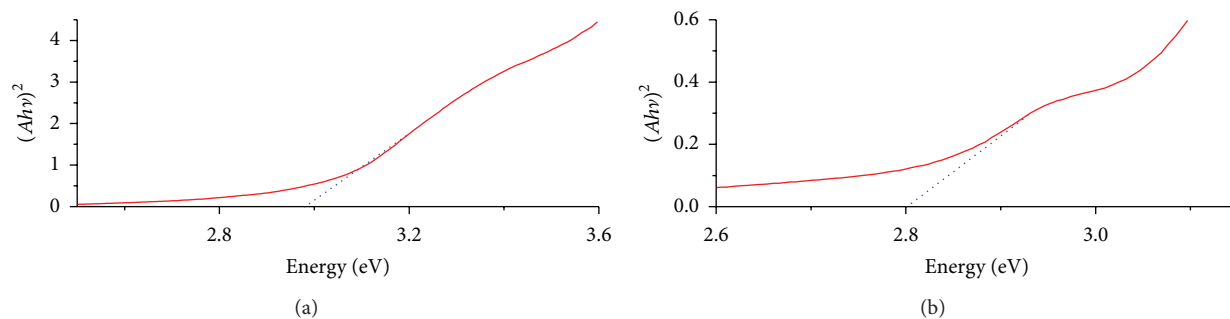


FIGURE 3: Absorbance squared $(Ahn)^2$ versus the photon energy (hn) extrapolated to zero absorption allows determination of optical band gap energy of BTE pigments. (a) Original pigment, (b) acidified pigment.

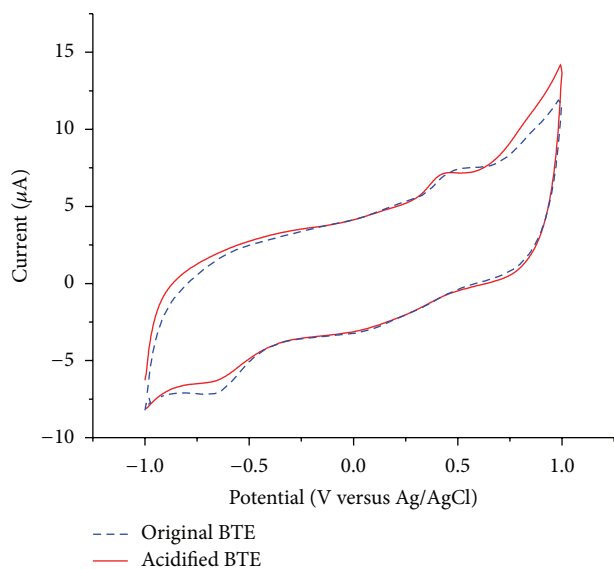


FIGURE 4: Cyclic voltammograms of BTE pigment (original and acidified).

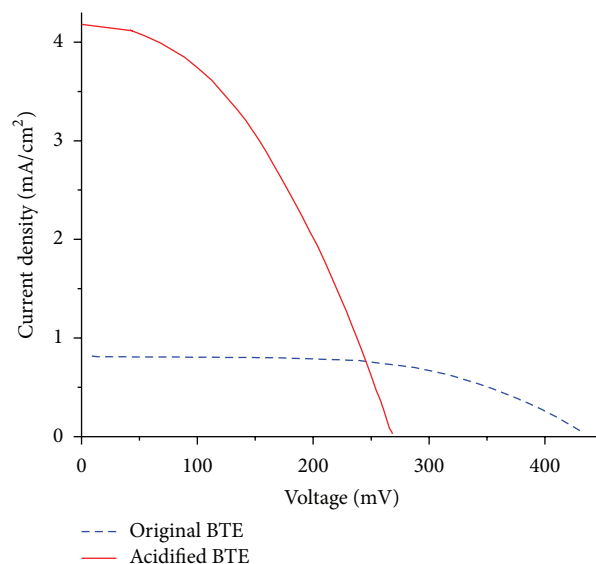


FIGURE 5: Comparison of I - V characteristics of the DSSCs sensitized with BTE pigment (original and acidified BTE).

TABLE 2: Photovoltaic characteristics of DSSCs sensitized with BTE pigments.

Pigment	I_{SC} ($mA\ cm^{-2}$)	V_{OC} (mV)	ff	$\eta\%$
BTE	0.82	434	0.57	0.2
Acidified BTE	4.21	268	0.41	0.46

enhanced by acidification of the pigment by 0.1M HCl. The acidified tea waste extract (pH = 3.5) as a sensitizer in DSSCs produced an overall efficiency of 0.46% with I_{SC} of $4.21\ mA\ cm^{-2}$ and V_{OC} of 268 mV. Further, the I - V characteristics of the DSSCs sensitized with BTE at various acidification conditions (pH = 2.5, 4.5) were investigated. The efficiencies showed by these DSSCs were almost the same as those of the DSSC sensitized with BTE at pH 3.5. At a basic condition (pH = 7) of BTE the efficiency was the same as the efficiency of DSSC sensitized with natural tea waste extract.

One reason for the enhancement of overall efficiency of the acidified pigment is due to its lower optical band gap compared to that of original BTE. In addition, the more

negativity of HOMO level upon lowering the pH of BTE enhances the donating ability of the pigment which directly affect the efficiency of the DSSC.

Furthermore, the original BTE has probably a low interaction between the pigment molecule and TiO_2 surface that leads to a reduced adsorption. This interaction is affected by the extracted pigment structure and its conformations. When the pigment was in acidic media, the adsorption properties of the pigment to TiO_2 may enhance resulting in increased performance of DSSCs [16].

3.4. Computational Studies. DFT and TDDFT computational studies produced in-depth insight in the energy levels and the simulated absorbance spectra of individual TF analogues. This information assessed the capability of the pigments as potential sensitizers. DFT and TDDFT data generated by computational studies show in Table 3.

DFT calculations were carried out with the inclusion of solvation effect of ethanol. The effect of hydrochloric acid cannot be included in the computational studies due to

TABLE 3: DFT and TDDFT calculations of four theaflavin analogues with inclusion of solvation effect of ethanol.

Tea polyphenol	DFT calculation			TDDFT calculation (excitation state $n = 3$)			
	HOMO (eV)	LUMO (eV)	Band gap (eV)	Calculated energy (eV)	Calculated energy (nm)	Oscillator strength (f)	MO (coefficient)*
TF	-5.32	-2.18	3.13	2.71	458	0.1005	H \rightarrow L = 0.675
				2.99	415	0.1754	H \rightarrow L + 1 = 0.667
				3.13	396	0.0001	H-1 \rightarrow L = 0.703
				2.83	439	0.0666	H \rightarrow L = 0.696
T3G	-5.61	-2.08	3.52	3.34	372	0.0005	H-1 \rightarrow L = 0.692
				3.42	363	0.0002	H-2 \rightarrow L = 0.635
				2.82	440	0.0502	H \rightarrow L = 0.669
				3.18	390	0.0002	H-1 \rightarrow L = 0.672
T3'G	-5.73	-2.21	3.52	3.31	374	0.0012	H-2 \rightarrow L = 0.682
				2.69	461	0.0908	H \rightarrow L = 0.683
				3.03	409	0.1937	H \rightarrow L + 1 = 0.672
TDG	-5.38	-2.23	3.15	3.16	393	0.0008	H-1 \rightarrow L = 0.700

*Molecular orbital with coefficient less than 0.2 is not shown.

the limitations of the software. As previously mentioned, effective injection of charge into conduction band of TiO_2 , the LUMO of the dye needs to be higher than the conduction band edge of TiO_2 . The computational generated energy levels of HOMO and LUMO of TF were -5.32 eV and -2.18 eV, respectively, whereas for TDG were -5.38 eV and -2.23 eV. Band gap of TF and TDG were 3.13 eV and 3.15 eV, respectively. The HOMO and LUMO values of T3G were -5.61 eV and -2.08 eV, whereas for T3'G were -5.73 eV and -2.21 eV. T3G and T3'G are isomers, and thus their energy levels were almost the same level which possessed the equal band gap of 3.52 eV. All the LUMO of the TFs were higher than the conduction band edge of TiO_2 , and the HOMO were more negative.

TDDFT calculation simulated the optical properties of the pigments. Three excitation states were included in TDDFT calculation. Oscillator strength is expressed by the strength of the transition of the pigment (e.g., from HOMO to LUMO). The higher the oscillator strength, the higher the potential of the pigment as a sensitizer [29]. At the first excitation state, the oscillator strengths of TF, T3G, T3'G, and TDG were 0.10, 0.07, 0.05, and 0.09, respectively, and all the four TFs showed a HOMO \rightarrow LUMO transition. The λ_{max} of TF, T3G, T3'G, and TDF were at 458 nm, 439 nm, 440 nm, and 461 nm, respectively (Figure 2(b)), and their computational generated energies were at 2.71 eV, 2.83 eV, 2.82 eV, and 2.69 eV.

At the second excitation state, the oscillator strength for the TFs were negligible, with the exception of TF and TDG at 0.18 and 0.19, respectively. Both TF and TDG involved HOMO \rightarrow LUMO + 1 transition, whereas T3G and T3'G involved HOMO - 1 \rightarrow LUMO transition. The computational generated energies of TF, T3G, T3'G, and TDG were 2.99 eV, 3.34 eV, 3.18 eV, and 3.03 eV.

At the third excitation state, all the TFs showed negligible oscillator strength. If excitation occurred at this state, TF and TDF would display HOMO - 1 \rightarrow LUMO transition, whereas T3G and T3'G display HOMO - 2 \rightarrow LUMO transition.

The computational generated energies of TF, T3G, T3'G, and TDG were 3.13 eV, 3.42 eV, 3.31 eV, and 3.16 eV.

TF and TDG have produced two significant oscillator strengths up to the second excitation state, while T3G and T3'G only produce significant oscillator strength at the first excitation states. This suggested that TF and TDG may be better sensitizers than T3G and T3'G. The peak height of the absorption spectra of TF and TDG is also higher than T3G and T3'G (Figure 2(b)) which indicated that TF and TDG have higher molar extinction coefficient.

3.5. Molecular Electronic Structure. Modelling of the electron clouds at various energy levels of the TFs was shown in Figure 6. At different energy levels, it can be observed that the electron clouds were localized at different regions of the molecule; however no delocalization was observed.

TF molecule consists of benzo-[7]-annulene (BA) unit and two catechin units. One catechin unit is attached to the benzene ring of the BA, while the other catechin unit is attached to the [7]-annulene unit of BA. At HOMO - 1, π -type electron clouds were localized on both catechin units. It can be observed from Figure 6 that the density of electron cloud is much higher at the catechin attached to the BA unit via benzene group. At HOMO, π -type electron cloud was localized at BA unit. Both LUMO and LUMO + 1 displayed π^* -type electron that was localized on BA unit.

T3G molecule is similar to theaflavin unit with an extra gallate unit (gallic acid unit). The gallate unit is attached to the catechin unit that is connected to the benzene of BA. T3G displayed π -type electron cloud for HOMO - 1 and HOMO. At HOMO - 1, electron cloud was localized on both catechin units. Higher density of electron cloud was observed to be localized on the catechin group attached to the benzene group of BA. At HOMO energy level, electron cloud shifted to the BA unit, leaving very small electron cloud on the catechin group. LUMO and LUMO + 1 displayed similar π^* -type electron cloud and was localized on the BA unit only.

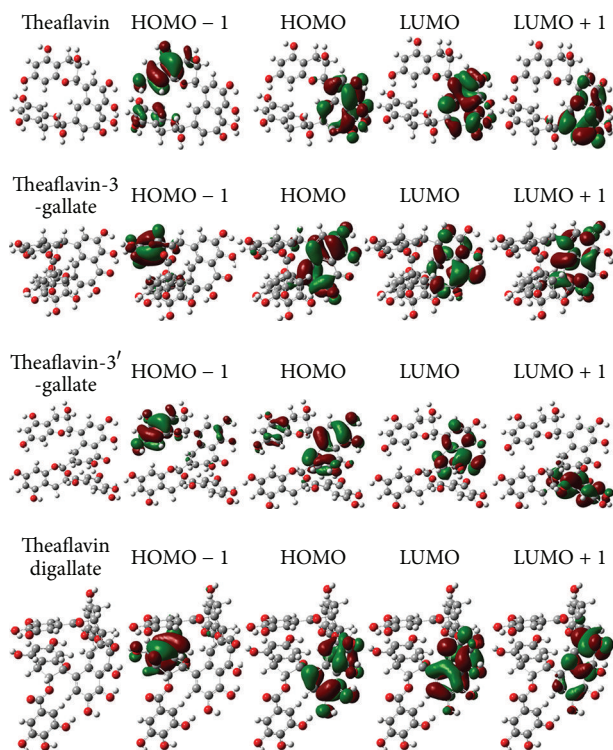


FIGURE 6: Modelling of the electron clouds of the four TF analogues at various transition states, plotted with isovalue of contour = 0.03.

T3'G molecule is an isomer of T3G. The gallate unit is attached to the catechin unit connected to BA via the [7]-annulene unit. At HOMO - 1, dense π -type electron cloud observed on catechin was connected to benzene unit of BA. Very small amount of electron cloud was observed on BA. At HOMO, it can be observed that there is a shift of electron cloud to the BA unit. Dense π -type electron cloud was observed at BA unit and very small amount on the catechin unit. LUMO displayed a π^* -type electron cloud, which was localized on BA unit. LUMO - 1 showed the shift of π^* -type electron cloud from the BA unit to the gallate unit. Very little electron cloud remained on the BA unit.

TDG is a large molecule containing a theaflavin unit and two gallate units. At HOMO - 1 energy level, dense π -type electron cloud localized in catechin unit was connected to benzene of BA; however at HOMO, there is a shift of π -type electron cloud to the BA unit. Both LUMO and LUMO - 1 displayed localization of π^* -type electron cloud at BA unit.

4. Conclusions

In summary, we fabricated DSSCs using pigment extracted from the black tea waste as the sensitizer, and the performance of the dye was reported. The best overall energy conversion efficiency of 0.46% was obtained from the extracted pigments at pH 3.5. The HOMO, LUMO levels and experimental optical band gaps of the black tea extract were calculated and determined using data from UV-vis absorption spectra and cyclic voltammetry. The enhancement

of overall efficiency of the acidified pigment is attributed to its enhanced adsorption properties, lowered optical band gap, and enhanced electron donating ability. From the DFT/TDDFT calculations, it was revealed that out of the four colored components of BTE only TF and TDG have the potential to sensitized DSSCs.

Conflict of Interests

The authors declare that there is no conflict of interests regarding the publication of this paper.

Acknowledgments

Universiti Brunei Darussalam (UBD) Research Grant UBD/PNC2/2/RG/1(176) and Brunei Research council Science and Technology Research Grant (S & T 17) are acknowledged for financial support.

References

- [1] K. Tennakone, G. R. R. A. Kumara, A. R. Kumarasinghe, P. M. Sirimanne, and K. G. U. Wijayantha, "Efficient photosensitization of nanocrystalline TiO_2 films by tannins and related phenolic substances," *Journal of Photochemistry and Photobiology A*, vol. 94, no. 2-3, pp. 217–220, 1996.
- [2] G. Calogero, G. Di Marco, S. Cazzanti et al., "Efficient dye-sensitized solar cells using red turnip and purple wild Sicilian prickly pear fruits," *International Journal of Molecular Sciences*, vol. 11, no. 1, pp. 254–267, 2010.
- [3] A. S. Polo and N. Y. Murakami Iha, "Blue sensitizers for solar cells: natural dyes from calafate and jaboticaba," *Solar Energy Materials and Solar Cells*, vol. 90, no. 13, pp. 1936–1944, 2006.
- [4] A. Hagfeldt, G. Boschloo, L. Sun, L. Kloo, and H. Pettersson, "Dye-sensitized solar cells," *Chemical Reviews*, vol. 110, no. 11, pp. 6595–6663, 2010.
- [5] A. S. Polo, M. K. Itokazu, and N. Y. Murakami Iha, "Metal complex sensitizers in dye-sensitized solar cells," *Coordination Chemistry Reviews*, vol. 248, no. 13-14, pp. 1343–1361, 2004.
- [6] G. P. Smestad and M. Grätzel, "Demonstrating electron transfer and nanotechnology: a natural dye-sensitized nanocrystalline energy converter," *Journal of Chemical Education*, vol. 75, no. 6, pp. 752–756, 1998.
- [7] G. K. R. Senadeera, T. Kitamura, Y. Wada, and S. Yanagida, "Photosensitization of nanocrystalline TiO_2 films by a polymer with two carboxylic groups, poly (3-thiophenemalonic acid)," *Solar Energy Materials and Solar Cells*, vol. 88, no. 3, pp. 315–322, 2005.
- [8] G. Calogero, J.-H. Yum, A. Sinopoli, G. Di Marco, M. Grätzel, and M. K. Nazeeruddin, "Anthocyanins and betalains as light-harvesting pigments for dye-sensitized solar cells," *Solar Energy*, vol. 86, no. 5, pp. 1563–1575, 2012.
- [9] M. Shahid, Shahid-ul-Islam, and F. Mohammad, "Recent advancements in natural dye applications: a review," *Journal of Cleaner Production*, vol. 53, pp. 310–331, 2013.
- [10] A. Gramza-Michalowska and J. Korczak, "Polyphenols-potential food improvement factor," *American Journal of Food Technology*, vol. 2, no. 7, pp. 662–670, 2007.
- [11] C. J. Dufresne and E. R. Farnworth, "A review of latest research findings on the health promotion properties of tea," *Journal of Nutritional Biochemistry*, vol. 12, no. 7, pp. 404–421, 2001.

- [12] S. V. Jovanovic, Y. Hara, S. Steenken, and M. G. Simic, "Antioxidant potential of theaflavins. A Pulse Radiolysis Study," *Journal of the American Chemical Society*, vol. 119, no. 23, pp. 5337–5343, 1997.
- [13] Y. Liang and Y. Xu, "Effect of extraction temperature on cream and extractability of black tea [*Camellia sinensis* (L.) O. Kuntze]," *International Journal of Food Science and Technology*, vol. 38, no. 1, pp. 37–45, 2003.
- [14] P. K. Mahanta and H. K. Baruah, "Theaflavin pigment formation and polyphenol activity as criteria of fermentation in orthodox and CTC teas," *Journal of Agricultural and Food Chemistry*, vol. 40, no. 5, pp. 860–863, 1992.
- [15] Y. Liang and Y. Xu, "Effect of pH on cream particle formation and solids extraction yield of black tea," *Food Chemistry*, vol. 74, no. 2, pp. 155–160, 2001.
- [16] M. R. Narayan, "Review: dye sensitized solar cells based on natural photosensitizers," *Renewable and Sustainable Energy Reviews*, vol. 16, no. 1, pp. 208–215, 2012.
- [17] K. Hara and H. Arakawa, "Dye-sensitized Solar Cells," in *Handbook of Photovoltaic Science and Engineering*, A. Luque and S. Hegedus, Eds., John Wiley & Sons, West Sussex, UK, 2003.
- [18] N. T. R. N. Kumara, P. Ekanayake, A. Lim, M. Iskandar, and L. C. Ming, "Study of the enhancement of cell performance of dye sensitized solar cells sensitized with nephelium lappaceum (F: Sapindaceae)," *Journal of Solar Energy Engineering*, vol. 135, no. 3, Article ID 031014, 2013.
- [19] N. T. R. N. Kumara, P. Ekanayake, A. Lim et al., "Layered co-sensitization for enhancement of conversion efficiency of natural dye sensitized solar cells," *Journal of Alloys and Compounds*, vol. 581, pp. 186–191, 2013.
- [20] B. Deppmeier, A. Driessen, T. Hehre et al., "Spartan'10," Wavefunction, 2011.
- [21] M. J. Frisch, G. W. Trucks, H. B. Schlegel et al., "Gaussian 09," Revision C.01, Gaussian, Wallingford, Conn, USA, 2010.
- [22] R. Dennington, T. Keith, and J. Millam, "GaussView," Version 5, Semichem, Shawnee Mission, Kan, USA, 2009.
- [23] S. Scharbert, N. Holzmann, and T. Hofmann, "Identification of the astringent taste compounds in black tea infusions by combining instrumental analysis and human bioresponse," *Journal of Agricultural and Food Chemistry*, vol. 52, no. 11, pp. 3498–3508, 2004.
- [24] A. Misra, P. Kumar, R. Srivastava, S. K. Dhawan, M. N. Kamalasanan, and S. Chandra, "Electrochemical and optical studies of conjugated polymers for three primary colours," *Indian Journal of Pure and Applied Physics*, vol. 43, no. 12, pp. 921–925, 2005.
- [25] J. Tauc, R. Grigorovici, and A. Vancu, "Optical properties and electronic structure of amorphous germanium," *Physica Status Solidi B*, vol. 15, no. 2, pp. 627–637, 1966.
- [26] F. N. Crespilho, V. Zucolotto, J. R. Siqueira, A. J. F. Carvalho, C. N. Francisco, and O. N. Oliveira, "Using electrochemical data to obtain energy diagrams for layer-by-layer films from metallic phthalocyanines," *International Journal of Electrochemical Science*, vol. 1, pp. 151–159, 2006.
- [27] G. P. Smestad, S. Spiekermann, J. Kowalik et al., "A technique to compare polythiophene solid-state dye sensitized TiO₂ solar cells to liquid junction devices," *Solar Energy Materials and Solar Cells*, vol. 76, no. 1, pp. 85–105, 2003.
- [28] H. Tian, X. Yang, J. Cong et al., "Effect of different electron donating groups on the performance of dye-sensitized solar cells," *Dyes and Pigments*, vol. 84, no. 1, pp. 62–68, 2010.
- [29] T. R. Heera and L. Cindrella, "Molecular orbital evaluation of charge flow dynamics in natural pigments based photosensitizers," *Journal of Molecular Modeling*, vol. 16, no. 3, pp. 523–533, 2010.



Hindawi

Submit your manuscripts at
<http://www.hindawi.com>

